Impact of initial damage path and spectral shape on aftershock collapse fragility of RC frames

Yang Liu[1,4a], Xiao-Hui Yu[*2,3,4], Da-Gang Lu[2,3,4b] and Fu-Zi Ma[4c]

[1]*College of Architecture and Environment, Sichuan University, Chengdu 610064, P.R. China*
[2]*Key Lab of Structures Dynamic Behavior and Control of the Ministry of Education, Harbin Institute of Technology, Harbin 150090, P.R. China*
[3]*Key Lab of Smart Prevention and Mitigation of Civil Engineering Disasters of the Ministry of Industry and Information Technology, Harbin Institute of Technology, Harbin 150090, P.R. China*
[4]*School of Civil Engineering, Harbin Institute of Technology, Harbin 150090, P.R. China*

Abstract. The influences of initial damage paths and aftershock (AS) spectral shape on the assessment of AS collapse fragility are investigated. To do this, a four-story ductile reinforced concrete (RC) frame structure is employed as the study case. The far-field earthquake records recommended by FEMA P695 are used as AS ground motions. The AS incremental dynamic analyses are performed for the damaged structure. To examine the effect of initial damage paths, a total of six kinds of initial damage paths are adopted to simulate different initial damage states of the structure by pushover analysis and dynamic analysis. For the pushover-based initial damage paths, the structure is "pushed" using either uniform or triangle lateral load pattern to a specified damage state quantified by the maximum inter-story drift ratio. Among the dynamic initial damage paths, one single mainshock ground motion or a suite of mainshock ground motions are used in the incremental dynamic analyses to generate a specified initial damage state to the structure. The results show that the structure collapse capacity is reduced as the increase of initial damage, and the initial damage paths show a significant effect on the calculated collapse capacities of the damaged structure (especially at severe damage states). To account for the effect of AS spectral shape, the AS collapse fragility can be adjusted at different target values of ε by using the linear correlation model between the collapse capacity (in term of spectral intensity) and the AS ε values, and coefficients of this linear model is found to be associated with the initial damage states.

Keywords: aftershock; mainshock; collapse fragility; damage path; spectral shape; RC frame structures

1. Introduction

It was frequency observed from the past earthquake events that a strong earthquake (referred to as 'mainshock', which is shortly denoted as MS hereafter) will typically trigger a sequence of aftershocks (denoted as AS hereafter). The MS-damaged structure is commonly not able to be repaired shortly after the MS due to the short time interval between the MS and the following ASs. Under such circumstance, the potential additional damage due to ASs may possess a significant threat to the structure damaged by MS.

Numerous studies had been conducted in the past in simulating nonlinear behaviors of single degree of freedom (SDOF) systems subjected to the MS-AS sequences in terms of ductility (Hatzigeorgiou 2010a, Goda and Taylor 2012), maximum displacement (Hatzigeorgiou and Beskos

2009), behavior factor (Hatzigeorgiou 2010b), damage index (Zhai *et al.* 2014), collapse capacity spectra (Yu *et al.* 2018), and failure probability (Iervolino *et al.* 2014). Recently, the more complex multi-story degree-of-freedom (MDOF) systems have also been used to assess the influences of MS-AS sequences on structural performance. The available studies covered reinforced concrete (RC) frames with (Tesfamariam *et al.* 2015) and without infilled walls (Faisal *et al.* 2013), steel frames (Ruiz-García and Aguilar 2017), wood frames (Goda and Salami 2014), steel bridges (Tang *et al.* 2016), steel arch bridges (Li *et al.* 2017), and ancient multi-drum columns (Papaloizou *et al.* 2016). Such studies using SDOF and MDOF systems have both revealed that the earthquake sequences can result in larger structural deformation comparing to that owing to individual earthquakes, which highlights the significance of accounting for AS effects in common seismic performance assessment of structures.

For a building damaged under a given earthquake sequence, it will experience two nonlinear stages, i.e., the intact building under the MS excitation and the MS-damaged structure subjected to the following ASs. Comparing to the first stage, the second is more complicated because of the accumulation of damage and the underlying physical mechanism. Increasing efforts have been made to investigate the residual capacity for an MS-damaged building (which is also referred as 'aftershock

---

*Corresponding author, Associate Professor
E-mail: xiaohui.yu@hit.edu.cn
[a]Ph.D.
E-mail: liuyang6886@163.com
[b]Professor
E-mail: ludagang@hit.edu.cn
[c]Postgraduate Student
E-mail: lmfoto@163.com

collapse capacity'). For example, Bazzurro (2006) proposed a simplified procedure for a quick evaluation of structural post-earthquake functionality in terms of fragility curves corresponding to different initial damage states, in which static pushover analyses are performed twice for the intact and damaged structure and then a SPO2IDA tool (Vamvatsikos and Cornell 2006) is used to infer dynamic response and determine the residual capacity of the damaged structure. Similar to Bazzurro (2006), a pushover-based method to estimate the residual capacity of the MS-damaged structure and derive damage-dependent vulnerability curves has been proposed and applied to RC frame structures (Polese *et al.* 2013), in which pushover analyses were also required to be performed twice for the intact and damaged structure. For the damaged structure, the force-deformation or moment-curvature relationships of structural elements should be modified according to the available experimental data (Polese *et al.* 2013). The incremental N2 (IN2) method (Dolšek and Fajfar 2004) was then used to define the collapse intensity as the median value of damage-dependent collapse function.

The afore-mentioned pushover-based strategies are quite simple and thus benefit the quick post-earthquake safety assessment; however, Luco *et al.* (2004) observed that the static analysis method in Bazzurro (2006) tends to underestimate the median residual capacity as compared with a more accurate approach called "back-to-back dynamic analysis method (Ryu *et al.* 2011)". Unlike the static analysis approach, the dynamic analysis method requires two incremental dynamic analyses (IDA), namely, one is performed by scaling the MS record to trigger a specified level of structural damage, while the other is conducted for scaling AS records until the damaged structure reaches the collapse state. This dynamic analysis method has been widely used in recent studies. For example, Ryu *et al.* (2011) developed aftershock collapse fragility curves for a typical RC frame structure located in New Zealand. As a companion study, Uma *et al.* (2011) examined the difference between the AS collapse fragility curves of the RC frame structures designed in accordance with New Zealand and US codes. These two studies both adopted the idealized SDOF systems by reducing the computation efforts; however, such treatment may result in considerable model errors that affects the accuracy of results. Therefore, more sophisticated and accurate MDOF systems were used in dynamic analyses to derive the AS collapse fragility curves. The relevant studies can be found for various structure systems, including steel frame structures (Li *et al.* 2014), wood frames (Nazari *et al.* 2013), modern RC frames (Raghunandan *et al.* 2015), non-ductile RC frame structures (Abdelnaby *et al.* 2015, Gaetani D'aragona *et al.* 2017) and infilled RC frames (Burton *et al.* 2017). These studies have revealed that structural damage owing to MS excitations will result in an increase of structural collapse probability. Specifically, if the MS-induced damage is severe, the structure is prone to high collapse potential even being subjected to an AS with minor amplitude.

For an intact structure experienced an MS excitation, it may suffer different levels of structural damage. Therefore,

a critical step in AS collapse fragility assessment is to simulate the specified initial damage states for the intact structure. In this step, two key issues should be addressed, including the quantification of the considered damage states and loading paths used to trigger initial damage (which is termed as 'initial damage path' hereafter). In the previous studies, different physical damage indictors have been used to quantify MS damage states and the correlation between damage indicators and the reduction of AS collapse capacity were established (Raghunandan *et al.* 2015, Burton *et al.* 2017). For the initial damage path, it is observed to be gradually dependent on the AS collapse capacity with the aggregation of initial structural damage (Li *et al.* 2014, Raghunandan *et al.* 2015). However, such conclusion is derived only considering the effect of randomness of MS records. Actually, to simulate a specific level of structural damage, pushover analysis (which requires less computation effect than that of IDA) can be used as an alternative analysis technique (Bazzurro 2006, Polese *et al.* 2013). To the best knowledge of the authors, only the idealized SDOF system has been used to compare the AS collapse capacity under pushover- and IDA-based initial damage paths (Luco *et al.* 2004). Therefore, it is valuable to conduct a comprehensive and thorough investigation on the influence of different initial damage paths on AS collapse fragility functions relying on sophisticated and accurate MDOF systems.

As an important characteristic of the AS record, the spectral shape of AS (Zhu *et al.* 2017) should be well considered when performing the AS-IDA (Goda 2015) and developing AS collapse fragility curves (Raghunandan *et al.* 2015). Li *et al.* (2014) observed a significant effect of AS spectral shape on the AS collapse fragility curves of steel frame structures. Then, the method proposed by Haselton *et al.* (2009) and recommended by FEMA (2009) has been used to adjust the derived AS collapse fragility with respect to the target spectral shape which is quantified by epsilon (ε). However, there are no related studies reported for the other types of structures. In addition, AS fragility assessment correlate closely with the initial damage states, while the dependence between the effect of AS spectral shape and the initial damage states has not been well examined. Therefore, more efforts are needed to incorporate AS spectral shape into the AS collapse fragility assessment for different types of MDOF systems,

The main objective of this study is to investigate the effects of initial damage path and AS spectral shape on AS collapse fragilities of ductile RC frame structures. A total of six types of initial damage paths due to static and dynamic analyses are considered. In particular, the intact structure can be defined having a given damage level through pushover analysis and IDA with and without considering the variability of MS records. Effect of AS spectral shape is considered in the development of AS collapse fragility curves by adjusting the corresponding model parameters in accordance with Haselton *et al.* (2009) and FEMA (2009). Based on the simulated results, the influences of initial damage paths and AS spectral shape on AS collapse capacity are quantified. The results could provide the valuable reference for AS collapse fragility analysis and
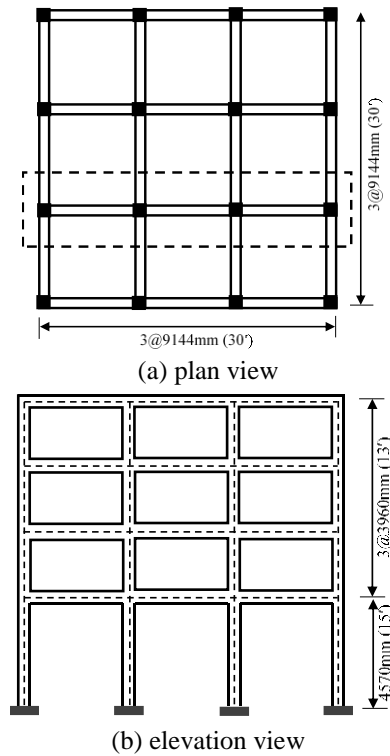
(a) plan view

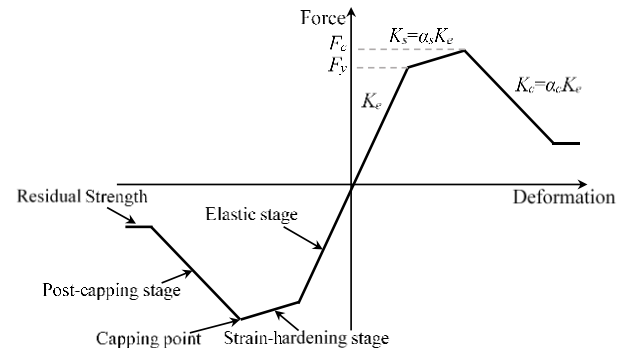(b) elevation view

Fig. 1 The case-study frame structure

Fig. 2 The backbone curve for the hysteresis model proposed by Ibarra *et al*. (2005)

Table 1 Model information of the studied RC frames using OpenSees

Objective	Model	Description
Beam	Lumped plastic hinge	The model developed by Ibarra *et al*. (2005) is used to account for both strength and stiffness deterioration
Column		
Joint	Elastic	Joint response is considered very small
P-Δ effect	Leaning column	A leaning column is set for the structural model with applying the gravity loads
Damping	Raleigh damping	Damping is modeled with 5% Rayleigh damping applied in the first and third modes of the structure

could benefit the post-earthquake safety assessment of structures.

2. Methodology

2.1 MS-AS earthquake sequences

Selection or synthesis of representative ground motion records to model structural collapse is a critical and challenging issue for the simulation of structural collapse due to earthquakes (Haselton *et al.* 2009). As discussed by Goda (2015), AS collapse fragility is significantly affected by the characteristics of AS records. In this study, two suites of artificial MS-AS earthquake sequences are used for the analysis. The sequence suites are generated using the ATC63 (FEMA 2009) far-field ground motion records as MS seeds and it includes a total of 44 horizontal records (two records each from the 22 earthquakes). The methodology on the selection of ATC63 far-field ground motion records and detail information regarding the selected records can be seen from FEMA (2009). Based on the selected MS seeds, the randomized method (Li and Ellingwood 2007) and the repeated method are used to synthesize the AS records. According to the randomized method, the AS records are randomly selected from the seeding MS records. For the repeated method, the AS records are generated by repeating the MS records.

2.2 A Ductile RC frame building

A typical ductile RC frame structures developed by Haselton *et al.* (2007) was adopted as the study case in this

paper. For completeness, essential structural design information is presented herein. The other design details regarding ID 1010 can be referred to Haselton *et al.* (2007). This frame has a total of four stories and was designed as a space frame according to the modern US design provisions (ASCE 2002, ACI 2002). Fig. 1 presents the plan and elevation arrangement of the case-study frame, where an identical bay width of 9144 mm (30′) was adopted and the first and other story heights are determined being 4570 mm (15′) and 3962 mm (13′), respectively. The column sizes are all 762 mm(30″)×762 mm (30″). The beam sizes are 762 mm(30″)×762 mm (30″) for the first two stories and 609 mm(24″)×762 mm (30″) for the other stories. The calculated fundamental period of this frame is T_1=0.86 sec. This frame was representative of the modern low-rise RC building located in the high-seismicity region of California. This frame was prone to experience significant earthquakes and it was thus valuable to examine the deterioration of its performance under ASs.

The RC frame was modeled by a two-dimensional and three-bay nonlinear model on OpenSees platform (Mazzoni *et al.* 2006). The model details can be referred to Haselton *et al.* (2007). For completeness, some crucial model issues are summarized in Table 1. In the structural model, the flexural behavior of beams and columns was modeled using lumped plastic hinge elements. A thorough consideration of element strength and stiffness deterioration is essential in simulating structural collapse due to earthquakes (Haselton *et al.* 2007). Therefore, a hysteresis model developed by
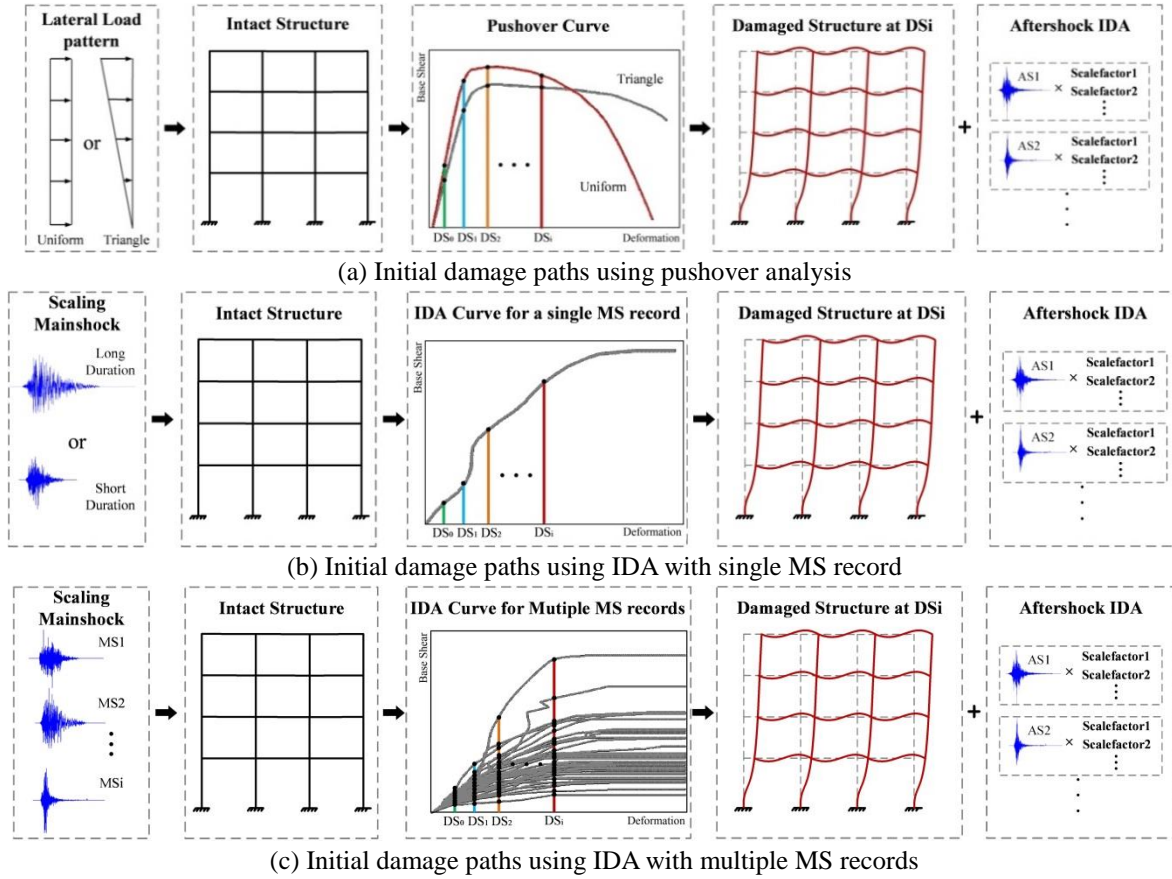
(a) Initial damage paths using pushover analysis

(b) Initial damage paths using IDA with single MS record

(c) Initial damage paths using IDA with multiple MS records

Fig. 3 Different initial damage paths used for AS collapse fragility assessment

Ibarra *et al*. (2005) was adopted herein to simulate the nonlinear behaviors of plastic hinge elements due to the advantages of the model in accounting for strength and stiffness deterioration. This hysteretic model could well account for all important deterioration sources of both strength and stiffness, including 1) strength deterioration in the post-capping range; 2) deterioration of unloading stiffness; and 3) deterioration of reloading stiffness. Fig. 2 shows the monotonic backbone curve of the hysteresis model, which consists of an elastic stage, a strain-hardening stage, a softening stage and a residual strength branch. The elastic stage is defined by the elastic stiffness K_e and the yield strength F_y. The strain-hardening stage with a stiffness, $K_s=\alpha_s K_e$, is capped at the maximum strength F_c. The softening stage is defined by the post-capping stiffness, $K_c=\alpha_c K_e$. The residual strength is defined as a fraction of the initial yield strength. Four energy dissipation-based rules are included in the hysteresis model to describe the cyclic deterioration of basic strength, post-capping strength, accelerated stiffness and unloading stiffness. Moreover, the pinching effect can also be included in the hysteretic model by introducing the pinching factors for force and deformation, respectively. Haselton (2008) has derived a suite of empirical equations to predict the backbone parameters based on a total of 255 calibrations of flexure-shear column tests. These derived empirical equations well correlate the design variables, such as, axial load, strengths of concrete and steel materials, reinforcements and confinements, etc., with the hysteresis model backbone

parameters. Using these equations, the plastic hinge backbone parameters are determined for all the columns and beams of the case-study RC frame. The specific values of the plastic hinge parameters are not presented herein for brevity but can be referred to Fig. 6.6 of Haselton *et al*. (2007).

Since the concerned frame was a modern designed one, its main failure mode due to an earthquake is a flexural failure, while the shear-induced brittle failure mode was not considered. In addition, the beam-column joints were assumed to respond elastically, which is based on the observations that well designed beam-column joints usually (and will) have the smaller response. The *P*-Δ effect is accounted for by applying gravity loads on a leaning column in the analysis model. A 5% Rayleigh damping model is used for the simulation of damping.

2.3 Initial damage paths

There are a total of three major steps to perform AS collapse fragility analysis for a given structure: 1) the intact structure is defined with different initial damage states; 2) the damaged structure is subjected to the AS records and AS-IDA curves are obtained; 3) the AS collapse capacities are derived from the AS-IDA curves and AS collapse fragility curves are generated. In the first step, six different initial damage paths due to static and dynamic analysis are considered herein to examine their effects on AS collapse fragilities, as shown in Fig. 3. Table 2 summarizes the

Table 2 The initial damage paths considered in this study

Path No.	Descriptions	Characteristics
DP-1	Pushover-induced damages with applied different lateral load patterns	Uniform lateral load pattern
DP-2		Triangle lateral load pattern
DP-3	IDA-induced damages without considering the variability of MS records	Using a MS record with a long duration
DP-4		Using a MS record with a short duration
DP-5	IDA-induced damages considering the variability of MS records	Using the MS records from the artificial MS-AS sequences by the repeated method
DP-6		Using MS records from the artificial MS-AS sequences by the randomized method

considered initial damage paths. Both the static (i.e., Pushover) and dynamic (i.e., IDA) procedures are used in the considered initial damage paths. Fig. 3(a) shows the initial damage paths simulated by the static methods, where pushover analysis is conducted at first on an intact structure to generate different levels of damages. Then AS-IDA can be performed for the damaged structure to determine the AS collapse capacity. Actually, the structural pushover curve is strongly affected by the lateral load patterns applied. Therefore, two types of lateral load patterns, the 'uniform (corresponding to SP-1 in Table 1)' and 'triangle (corresponding to SP-2 in Table 1)', are used to generate the initial damages. For the uniform pattern, the lateral forces are proportional to the local masses at each floor level, while the accelerations are proportional to the story heights in the triangular load pattern.

Besides the static procedure, the dynamic is also used to generate the specified initial damage states and Fig. 3(b) presents the considered two initial damage paths (DP-3 and DP-4) based on the dynamic methods, where only a single MS record is used to produce the initial damages (meaning that effect of variability of MS records is not considered). Since the duration of a ground motion is also an important seismic characteristic relevant to structural damages, the MS records having a long and short duration are used in DP-3 and DP-4, respectively. Fig. 3(c) presents the initial damage paths due to multiple MS records to investigate the effect of MS variability on AS collapse fragilities. In this study, two suites of artificial MS-AS sequences are generated by the repeated method and the randomized method (Section 2.1) and are used for DP-5 and DP-6, respectively. Under a given initial damage state, the AS collapse fragility curves under different initial damage paths are compared to investigate the influences of the considered initial damage paths on the AS collapse capacity.

2.4 Adjustment of AS collapse fragility accounting for AS spectral shape

The spectral shape has been observed to significantly affect the collapse capacity of structures (FEMA 2009). To measure the difference of spectral shape, epsilon, ε, is commonly used as an indicator that is defined as the

standardized difference between a given value of $\ln S_a$ and the predicted mean value of $\ln S_a$ through the ground motion predictive equation. The mathematical formula of ε can be expressed as (Baker and Cornell 2005)

$$\varepsilon(T) = \frac{\ln S_a(T) - \mu_{\ln S_a}(M,R,T)}{\sigma_{\ln S_a}(T)} \quad (1)$$

where T is a specified spectral period; M and R are the given magnitude and distance, respectively; and $\mu_{\ln Sa}$ and $\sigma_{\ln Sa}$ are the predicted mean and standard deviation of $\ln S_a$ for the given M and R, respectively, from the ground motion predictive equation.

Because of the significant influence of ε on structural collapse capacity, the effect of ε on seismic collapse analysis is studied. In this study, the method proposed by Haselton *et al.* (2009) in adjusting the calculated collapse fragility to incorporate the effect of ε is adopted to reflect the influence of AS spectral shape on AS collapse fragility. According to this method, $\varepsilon(T_1)$ values at the natural periods (T_1=0.94s for the studied RC frame) of the studied buildings are calculated firstly for each of the AS records, in which the ground motion predictive equation proposed by Abrahamson and Silva (2008) is adopted. Then, AS-IDA is performed for each AS record to obtain the corresponding collapse capacity based on spectral acceleration $S_a(T_1)$. A linear relationship between $S_a(T_1)$ and $\varepsilon(T_1)$ can be regressed(Liu *et al.* 2017), yielding

$$\ln S_a(T_1)=a_0+a_1\varepsilon(T_1) \quad (2)$$

where a_0 and a_1 are the regression coefficients and Eq. (2) represents the correlation between mean $\ln S_a(T_1)$ and $\varepsilon(T_1)$. Given a target $\varepsilon(T_1)$ value, the mean value of $\ln S_a(T_1)$ (corresponding to the median AS collapse capacity of an AS collapse fragility function) can be adjusted. It should be noted that, in addition to the adjustment of median collapse capacity, dispersion of collapse fragility function can also be reduced by accounting for the effect of ε. However, the degree of reduction is limited (Haselton *et al.* 2009) and is thus not considered herein for simplicity.

3. AS collapse fragility assessment using different initial damage paths

To quantify the initial structural damage, this study considers a total of six damage states from DS_1 to DS_6 in terms of the maximum inter-story drift θ_{max} being 1%, 2%, 3%, 4%, 5% and 6%, respectively. For a given initial damage state, IDA is performed on the damaged structure to generate IDA curves corresponding to each of AS records. The collapse state is defined as the $S_a(T_1)$ intensity level at which the structure becomes unstable, which corresponds to a point on an IDA curve followed with a flat line, as shown in Fig. 4. When evaluating AS collapse capacity, the AS records can be either positively or negatively scaled, which is commonly referred as the 'polarity' of AS (Ryu *et al.* 2011, Raghunandan *et al.* 2015). In this study, the polarity of AS is selected randomly since it is generally unknown in the real earthquake scenarios (Ryu *et al.* 2011, Raghunandan
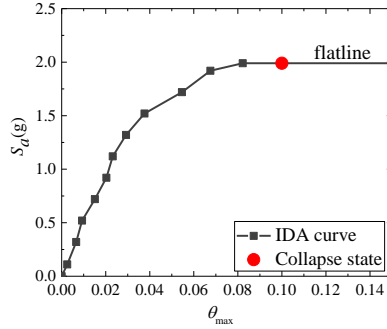
Fig. 4 Identification of collapse state on an IDA curve

et al. 2015).

A single initial damage path of DP-6 is adopted at first to examine the effect of initial damage states on AS collapse capacity. Fig. 5 shows the AS-IDA curves for the intact structure and the MS-damaged structures. For illustrate the effect of initial damage states clearly, the median AS-IDA curves are compared for the intact structure and the damaged structure with different initial damage states, as shown in Fig.6. As observed, the increase of initial damage will cause a clear reduction on the structural capacity to

resist aftershocks. In particular, for a given θ_{max} response, the required AS intensity for the severely damaged structure is significantly smaller than that for the slight damaged (or intact) structure. For the case of DS_1, its corresponding AS-IDA curve is close to the intact case due to its ignorable effect on the structural performance.

Collapse capacities are assumed to follow lognormal fragility function model that is defined by two parameters, i.e., a) the median collapse capacity, m_R; and b) the logarithm standard deviation (it is also referred as 'dispersion') of collapse capacity, β_R. Using the lognormal fragility function, the AS collapse fragility curves for the intact and damaged structures are derived and compared in Fig. 7(a). It is found that the intact structure has the least possibility of collapse for a given level of AS intensity $S_a(T_1)$ in comparison with the damaged structures. Moreover, the probability of collapse at a given AS intensity $S_a(T_1)$ is increased more for the structure with more severe damages. The effects of initial damage states on AS collapse fragilities can be further observed from the comparison of AS collapse fragility parameters between the intact and damaged structures, as shown in Fig. 7(b). As observed, a significant reduction of the median collapse capacity is induced by the increase of initial damage states.

(a) intact structure

(b) DS_1

(c) DS_2

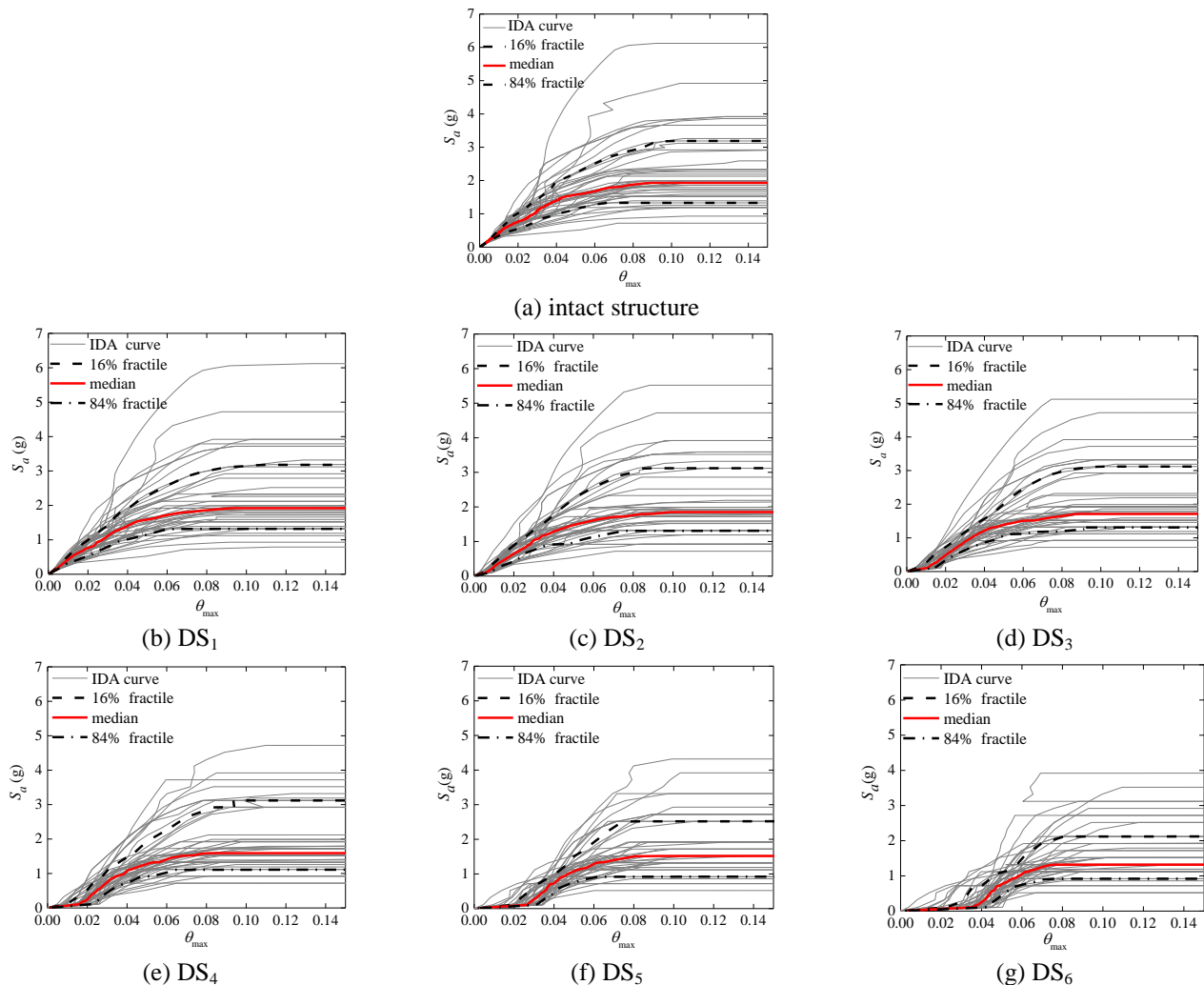
(d) DS_3

(e) DS_4

(f) DS_5

(g) DS_6

Fig. 5 AS-IDA curves for the four-story frame suffering different initial damage states
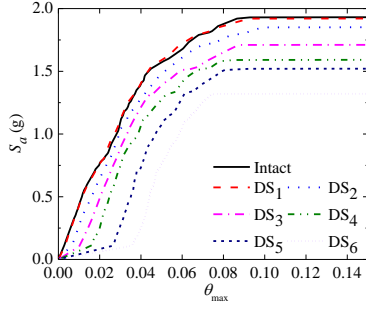
Fig. 6 Comparison of median IDA curves for the four-story RC frame suffering different damage states
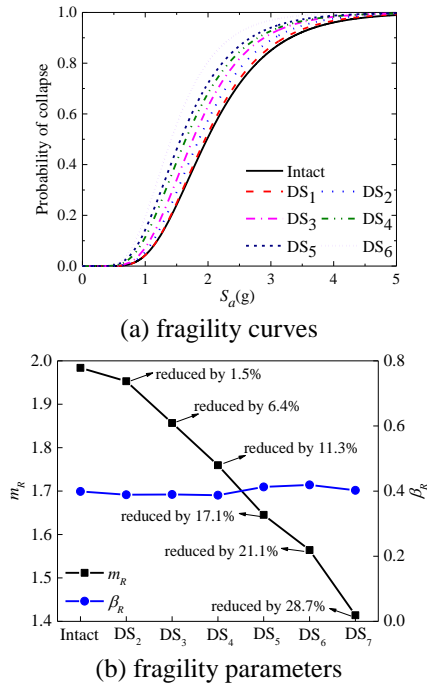

(a) fragility curves

(b) fragility parameters

Fig. 7 Effects of initial damage states on AS collapse fragility

In particular, the reduction percentage of m_R for the damaged structures at DS_1 ($\theta_{max}=1\%$) is only 1.5%, while it is greatly increased above 10% when the initial damage of the structure reaches $\theta_{max}=3\%$. If the initial damage reaches DS_4, the resulting reduction of m_R is close to 20%. Such reduction scale should be well considered in the post-earthquake safety assessment of structures. Unlike m_R, the dispersion β_R of collapse fragility is not significantly affected by the initial damages, and there is no clear trend observed for the β_R value as the increase of initial damage states.

Next, effects of initial damage paths on AS collapse fragilities are examined. The AS-IDA curves are generated first using the considered six types of initial damage paths to generate different levels of initial damage. Fig. 8 illustrates the AS-IDA curves for the RC frame with a moderate damage level of DS_4. From the obtained AS-IDA curves, the S_a intensities corresponding to the collapse state are captured for each AS record, and the lognormal collapse fragility curves are developed and are shown in Fig. 9. The fragility parameters of m_R and β_R are calculated for each
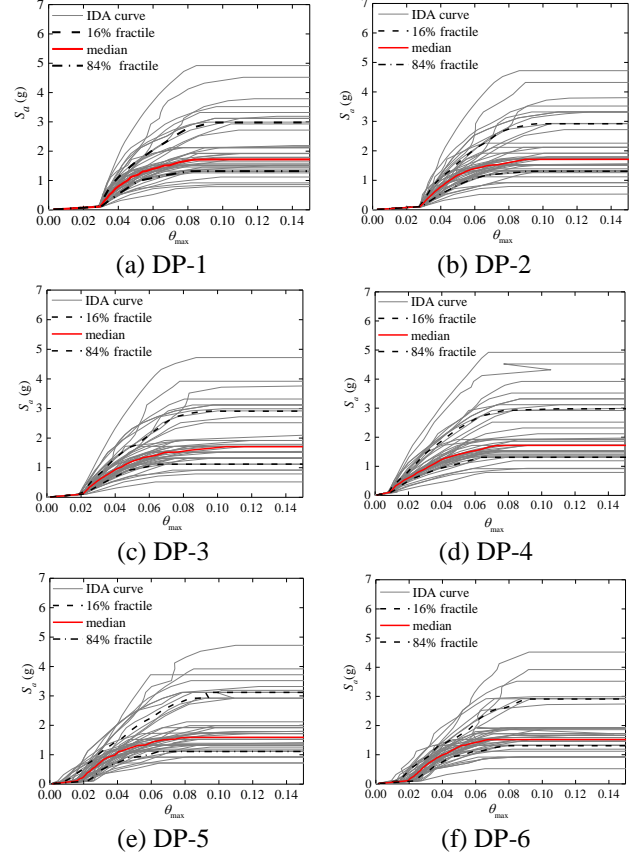

(a) DP-1 (b) DP-2

(c) DP-3 (d) DP-4

(e) DP-5 (f) DP-6

Fig. 8 IDA curves for the four-story RC frame with DS_4 due to different initial damage paths

(a) DP-1 (b) DP-2

(c) DP-3 (d) DP-4

(e) DP-5 (f) DP-6
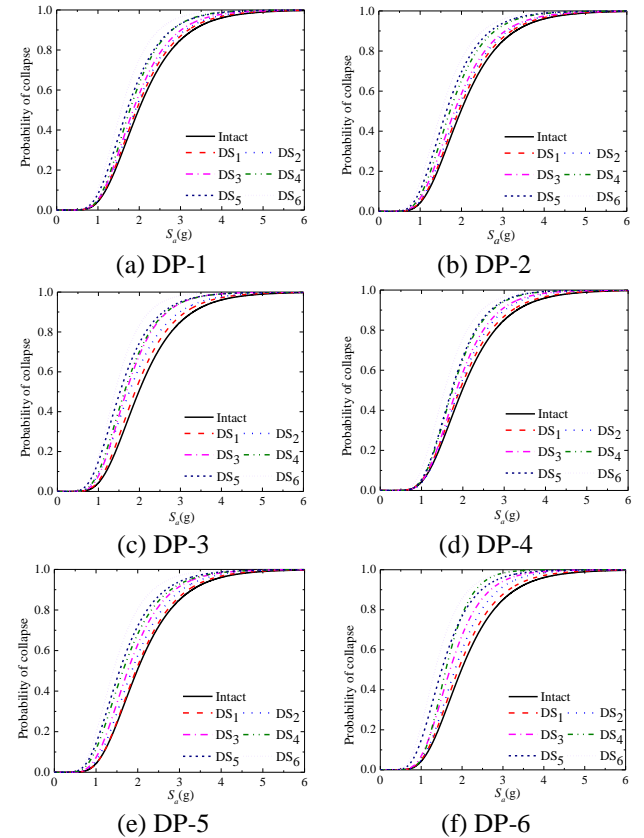
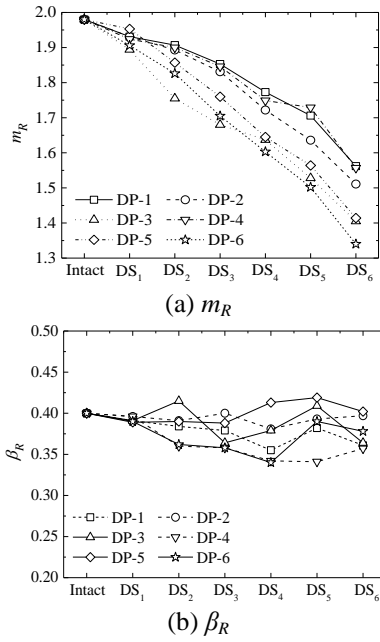Fig. 9 AS collapse fragility curves for the intact of damaged four-story RC frame considering different damage paths

(a) m_R

(b) β_R

Fig. 10 Effects of initial damage paths on AS collapse fragility parameters

Fig. 11 Histogram of ε values for AS records

initial damage path and the calculated results are shown in Fig. 10(a) and Fig. 10(b), respectively. The initial damage paths exhibit evident effect on the results of m_R and such effect tends to be magnified as the increase of initial damages of structures.
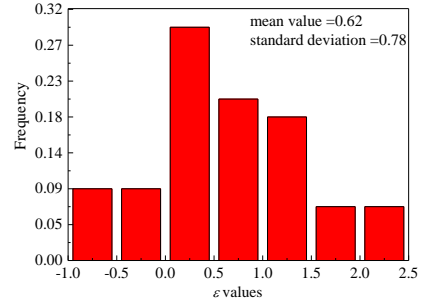
Among the considered initial damage paths, DP-6 results in the largest reduction on the median collapse capacity of the structure, especially at the severe initial damage states, i.e., DS$_4$, DS$_5$ and DS$_6$. Compared to DP-6, DP-5 shows considerably less effect on the values of m_R at different initial damage states, indicating that the synthesis methods of artificial earthquake sequences have significant effects on the assessment of AS collapse fragility. The initial damage states of DP-1 and DP-4 can result in almost identical effects on median collapse capacity but the smallest effects comparing to that by the other initial damage states. Compared to DP-1 results, DP-2 results in the larger decrease in the median collapse capacity. This shows that, given a specified initial damage state, the pushover procedure using a uniform lateral load pattern can cause the structure more vulnerable to the ASs than that using a triangle lateral load pattern.
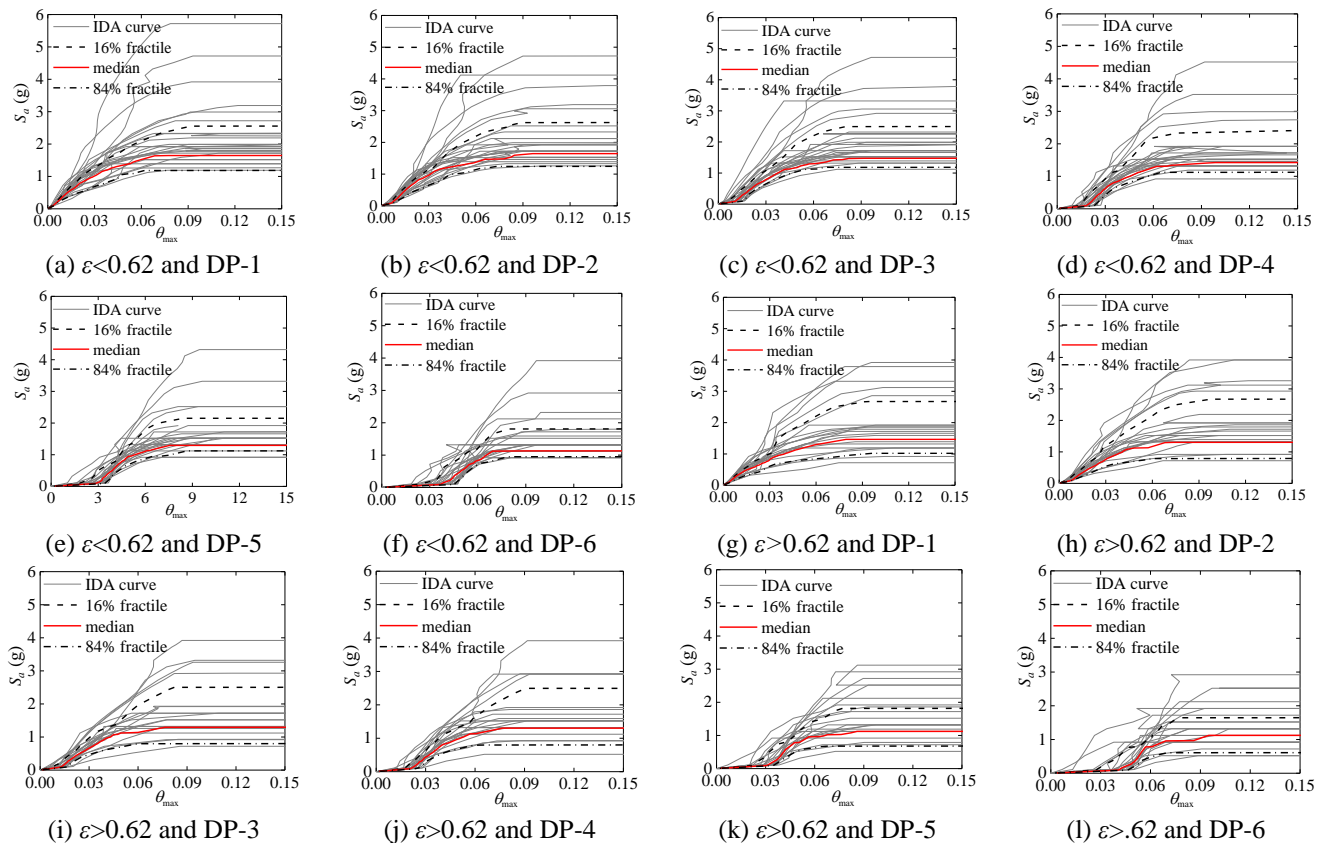

(a) $\varepsilon<0.62$ and DP-1

(b) $\varepsilon<0.62$ and DP-2

(c) $\varepsilon<0.62$ and DP-3

(d) $\varepsilon<0.62$ and DP-4

(e) $\varepsilon<0.62$ and DP-5

(f) $\varepsilon<0.62$ and DP-6

(g) $\varepsilon>0.62$ and DP-1

(h) $\varepsilon>0.62$ and DP-2

(i) $\varepsilon>0.62$ and DP-3

(j) $\varepsilon>0.62$ and DP-4

(k) $\varepsilon>0.62$ and DP-5

(l) $\varepsilon>.62$ and DP-6

Fig. 12 IDA curves for the damaged structure using the AS records belonging to different groups of $\varepsilon<0.62$ and $\varepsilon>0.62$

(a) $\varepsilon < 0.62$
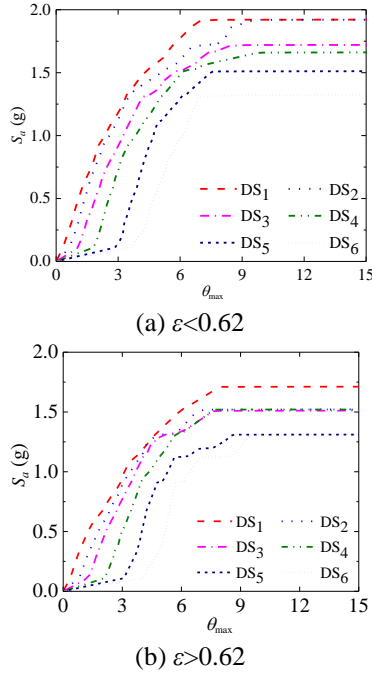

(b) $\varepsilon > 0.62$

Fig. 13 Median IDA curves by the AS records with different ε values

Moreover, the duration of MS record is also an essential factor affecting the AS collapse fragility. For a given initial damage state, the MS with long duration can increase the damage potential of the structure when it is subjected to the following AS records. This is attributed to the fact that ground motion record with longer duration has larger
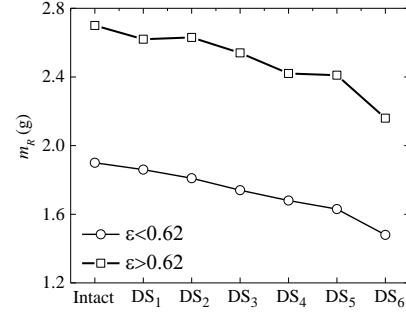

Fig. 14 Comparison of m_R values calculated from the AS records belonging to different ε groups

seismic energy than that with shorter duration. Unlike m_R, there is no obvious effect as observed on β_R values owing to different initial damage paths. This β_R values corresponding to different initial damage states approximately vary from 0.35 to 0.40.

4. AS collapse fragility assessment considering AS spectral shape

This section mainly investigates the effects of AS spectral shape on the assessment of AS collapse fragility. To do this, the ε values at $T_1 = 0.93$s for the studied frame are preliminarily calculated for each AS record according to Eq. (1). Fig. 11 shows the histogram of the calculated AS ε values, with the mean value of 0.62 and the standard deviation of 0.78. Then the AS records are categorized into two groups, which are $\varepsilon(0.93s) < 0.62$ and $\varepsilon(0.93s) > 0.62$.
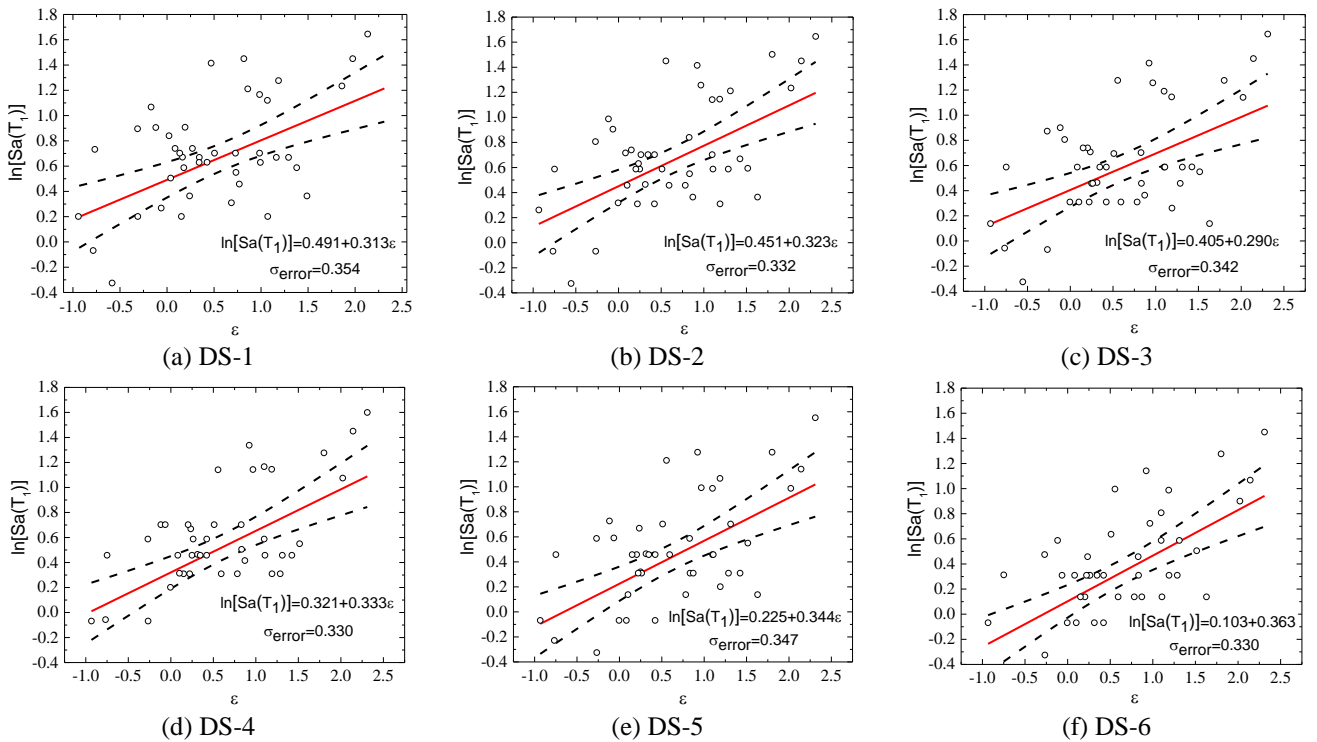

(a) DS-1

(b) DS-2

(c) DS-3

(d) DS-4

(e) DS-5

(f) DS-6

Fig. 15 Relationship between the collapse capacity quantified by an intensity of spectral acceleration and ε values for each AS record and the linear regressions between $\ln S_a$ and ε considering different initial damage states
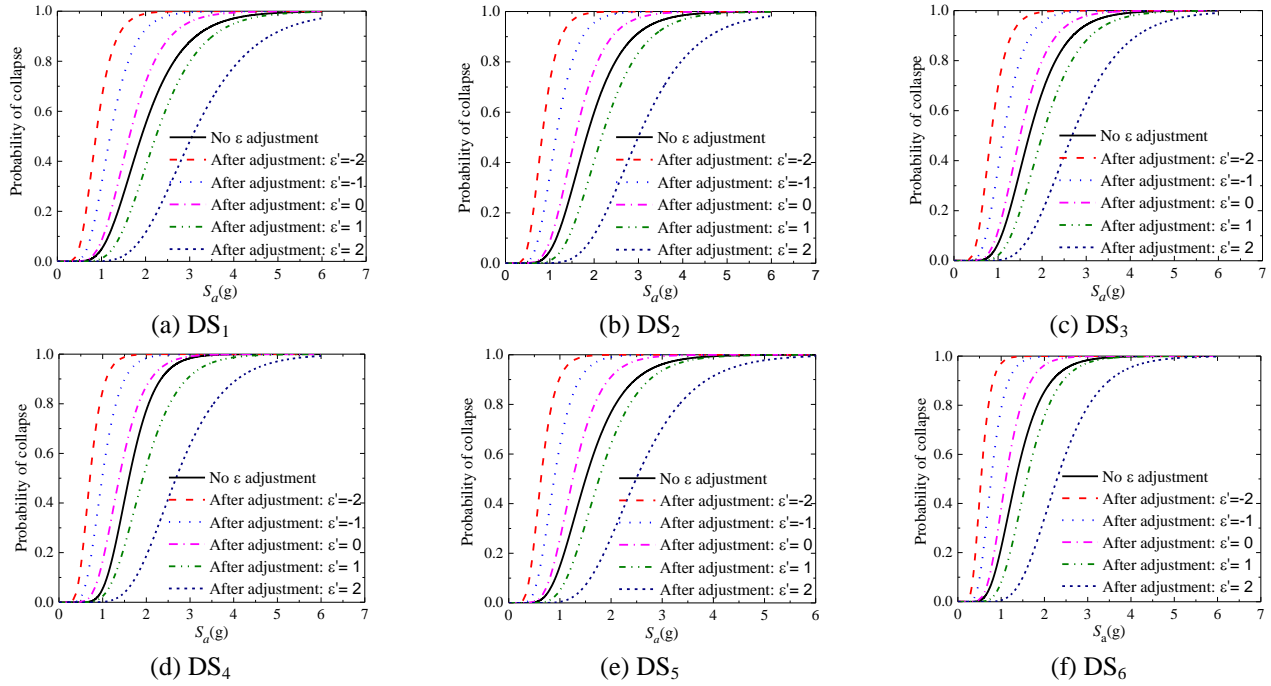
Fig. 16 Comparison of the AS collapse fragility curves with and without considering ε adjustment for the damaged structure at different initial damage states

These two groups of AS record are used to generate AS-IDA curves separately for the damaged structure at different initial damage states, as shown in Fig. 12.

Since the main focus of this study is to examine the effect of AS spectral shape, only the initial damage path of DP-6 is used herein. It is observed that AS spectral shape shows the evident effect on AS-IDA curves when comparing the median IDA curves from different AS record group as shown in Fig. 13. The dependence between AS spectral shape and AS collapse capacity reveals the considerable effect of AS spectral shape on AS collapse fragility. Fig. 14 shows the comparison of m_R values due to different groups of AS records with $\varepsilon(0.93s)<0.62$ and $\varepsilon(0.93s)>0.62$, and it is clearly seen that the median collapse capacity is significantly affected by the AS ε values. Therefore, it is necessary to modify the obtained AS fragility by considering the effect of AS spectral shape. According to the methodology proposed by Haselton *et al.* (2009), the median collapse capacity is adjusted at the target ε value and dispersion of the fragility remains for simplicity.

Based on the AS-IDA curves, the intensities of S_a causing structural collapse are obtained for each AS record, which is further correlated to the ε values of AS records. The linear assumption (shown in Eq. (2)) is used to describe the dependence between S_a and ε, and the results are presented in Fig. 15. It should be noted that the linear regression results vary with the initial damage states. Therefore, the regression coefficients of a_1 and a_2 in Eq. (2) are also varying with the initial damage states (which will be discussed later). Based on the established linear relationship between $\ln S_a$ and ε, the median collapse capacity obtained without considering AS spectral shape is recalculated at varying values of ε. Fig. 16 shows the comparison of collapse fragility curves with and without
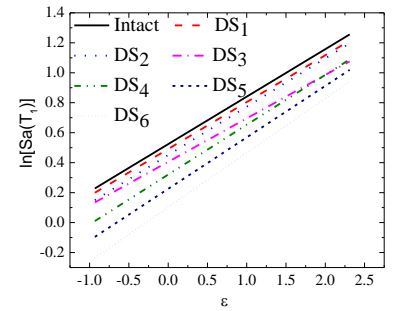
(a) Linear regressions
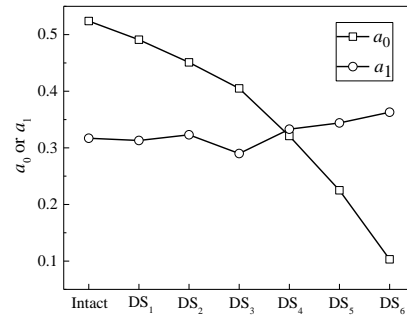
(b) Coefficients of regression

Fig. 17 Linear relationships between $\ln S_a(T_1)$ and ε varying along the initial damage states

considering the adjustment for AS spectral shape, where a suite of target values of ε, including ε'=(-2, -1, 0, 1, 2), are considered. It is clear that, as the increase of the target value of ε, the adjusted fragility curves are shifted towards to the right. Actually, the adjustment owing to the effect of AS spectral shape can greatly change the prediction of collapse probability for the MS-damaged structure under the potential AS strike.
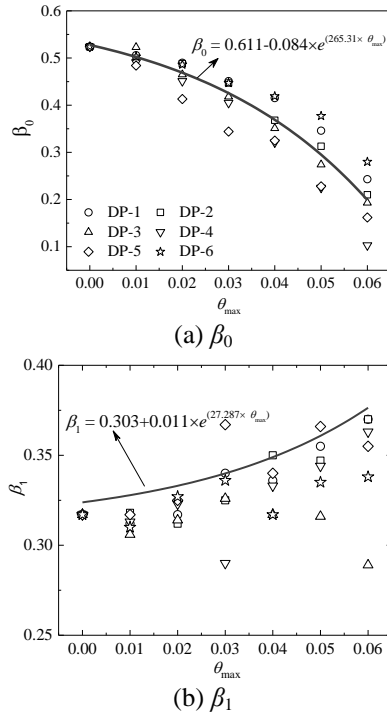
$$\beta_0 = 0.611 - 0.084 \times e^{(265.31 \times \theta_{max})}$$

	DP-1		DP-2
	DP-3		DP-4
	DP-5		DP-6

(a) β_0

$$\beta_1 = 0.303 + 0.011 \times e^{(27.287 \times \theta_{max})}$$

(b) β_1

Fig. 18 Relationship between the coefficients of β_0 and β_1 and the initial damages quantified by θ_{max}

It has been observed that the regressed linear relationship between the collapse capacity (in terms of $\ln S_a$ and the AS ε) for the damaged structure is affected by the initial damage states of the structure. Fig. 17(a) shows the regression results for the damaged structure at different initial damage states. There is a clear difference inherent on the regression results between different initial damage states. Therefore, the regression coefficients of a_0 and a_1 are varying with the initial damage states, as shown in Fig. 17(b). As observed, the a_0 values are decreased as the increase of structural initial damage, while the a_1 values are slightly increased accordingly. To quantify the observed trends for a_0 and a_1, two power-law functions are used to fit the values of a_0 and a_1 separately, which are given in Fig. 18(a) and Fig. 18(b), respectively. These fitted functions can also account for the effect of different initial damage paths and they can be further used to adjust the AS collapse fragility in a simplified and straightforward way.

5. Conclusions

A comprehensive and thorough investigation for the effects of initial damage paths and AS spectral shape on AS collapse fragility assessment has been conducted. The following conclusions can be drawn from this study:

(1) Initial damage states have significant effects on the AS collapse capacity of structures. The reduction percentage on median collapse capacity of the damaged structure ranges from less than 1.5% to more than 20% when the initial damage states vary from the slight damage to very severe damage. This findings consolidates the previous relevant studies that, when the

structure suffering from severe damage, its collapse potential due to ASs is greatly increased.

(2) Initial damage paths were proved to be another essential factor affecting the assessment of AS collapse fragility. For a given initial damage state quantified by a specified θ_{max}, the AS collapse fragility results are varying with the initial damage paths and such difference owing to different initial damage paths is magnified for structure with more damages.

(3) For the pushover-based damage paths, the one using the uniform lateral load pattern is observed causing the damaged structure more vulnerable to AS, comparing to that using the triangle lateral load pattern. For the damage paths using dynamic analysis, the MS ground motion with a longer duration was more destructive than that with a shorter duration, indicating that the input seismic energy is a curtail indicator of the MS-damage for the assessment of AS collapse fragility. For the cases considering the variability of MS ground motions, the synthesis methods of artificial MS-AS sequence significantly affect AS collapse fragility.

(4) The AS spectral shape was found to be a critical factor affecting AS collapse fragility. The method proposed by Haselton *et al.* (2009) was proven to be an efficient technique to account for the AS spectral shape by adjusting the median collapse capacity at different target value of ε. The linear relation model, as derived between the calculated AS collapse capacity (quantified by intensity S_a) and the ε values for each AS record, varies with initial damage states, and the regression coefficients can be approximately represented by the power-law functions.

(5) It is noteworthy that the current study is limited to one four-story RC frame structure. More study cases are needed in future to obtain the more comprehensive and robust conclusions on the AS collapse fragility assessment. However, the present study can still provide in-depth insight into the influence of initial damage paths and AS spectral shape on the AS collapse fragility assessment.

Acknowledgments

References

Abdelnaby, A.E. (2015), "Numerical modeling and analysis of rc frames subjected to multiple earthquakes", *Earthq. Struct.*, **9**(5), 957-981.

Abrahamson, N. and Silva, W. (2008), "Summary of the abrahamson & silva nga ground-motion relations", *Earthq. Spectra*, **24**(1), 67-97.

American Concrete Institute (ACI) (2002), "Building code requirements for structural concrete and commentary", ACI 318-02/ACI 318R-02, Farmington Hills, MI.

ASCE (2002), "Minimum design loads for buildings and other

structures", ASCE 7-02, Reston, VA.

Baker, J.W. and Cornell, C.A. (2005), "A vector-valued ground motion intensity measure consisting of spectral acceleration and epsilon", *Earthq. Eng. Struct. Dyn.*, **34**(10), 1193-1217.

Bazzurro, P. (2006), *Advanced Seismic Assessment Guidelines*, Pacific Earthquake Engineering Research Center.

Burton, H.V., Sreekumar, S., Sharma, M. and Sun, H. (2017), "Estimating aftershock collapse vulnerability using mainshock intensity, structural response and physical damage indicators", *Struct. Saf.*, **68**(85-96).

Dolšek, M. and Fajfar, P. (2004), "In2-a simple alternative for ida", *Proceedings of the 13th World Conference on Earthquake Engineering*, Vancouver, Canada.

Faisal, A., Majid, T.A. and Hatzigeorgiou, G.D. (2013), "Investigation of story ductility demands of inelastic concrete frames subjected to repeated earthquakes", *Soil Dyn. Earthq. Eng.*, **44**, 42-53.

Fema, P. (2009), "695. Quantification of building seismic performance factors", Federal Emergency Management Agency.

Gaetani D'aragona, M., Polese, M., Elwood, K.J., Baradaran Shoraka, M. and Prota, A. (2017), "Aftershock collapse fragility curves for non-ductile RC buildings: A scenario-based assessment", *Earthq. Eng. Struct. Dyn.*, **46**(13), 2083-2102.

Goda, K. (2015), "Record selection for aftershock incremental dynamic analysis", *Earthq. Eng. Struct. Dyn.*, **44**(7), 1157-1162.

Goda, K. and Taylor, C.A. (2012), "Effects of aftershocks on peak ductility demand due to strong ground motion records from shallow crustal earthquakes", *Earthq. Eng. Struct. Dyn.*, **41**(15), 2311-2330.

Goda, K. and Salami, M.R. (2014), "Inelastic seismic demand estimation of wood-frame houses subjected to mainshock-aftershock sequences", *Bull. Earthq. Eng.*, **12**(2), 855-874.

Haselton, C.B., Baker, J.W., Liel, A.B. and Deierlein, G.G. (2009), "Accounting for ground-motion spectral shape characteristics in structural collapse assessment through an adjustment for epsilon", *J. Struct. Eng.*, **137**(3), 332-344.

Haselton, C.B. and Deierlein, G.G. (2007), *Assessing Seismic Collapse Safety of Modern Reinforced Concrete Moment-frame Buildings*, Pacific Earthquake Engineering Research Center.

Haselton, C.B., Liel, A.B., Dean, B.S., Chou, J.H. and Deierlein, G.G. (2007), "Seismic collapse safety and behavior of modern reinforced concrete moment-frame buildings", *Am. Soc. Civil Eng.*, **249**, 1-14.

Hatzigeorgiou, G. (2010b), "Behavior factors for nonlinear structures subjected to multiple near-fault earthquakes", *Comput. Struct.*, **88**(5-6), 309-321.

Hatzigeorgiou, G.D. (2010a), "Ductility demand spectra for multiple near-and far-fault earthquakes", *Soil Dyn. Earthq. Eng.*, **30**(4), 170-183.

Hatzigeorgiou, G.D. and Beskos, D.E. (2009), "Inelastic displacement ratios for sdof structures subjected to repeated earthquakes", *Eng. Struct.*, **31**(11), 2744-2755.

Ibarra, L.F., Medina, R.A. and Krawinkler, H. (2005), "Hysteretic models that incorporate strength and stiffness deterioration", *Earthq. Eng. Struct. Dyn.*, **34**(12), 1489-1511.

Iervolino, I., Giorgio, M. and Chioccarelli, E. (2014), "Closed-form aftershock reliability of damage-cumulating elastic-perfectly-plastic systems", *Earthq. Eng. Struct. Dyn.*, **43**(4), 613-625.

Li, Q. and Ellingwood, B.R. (2007), "Performance evaluation and damage assessment of steel frame buildings under main shock–aftershock earthquake sequences", *Earthq. Eng. Struct. Dyn.*, **36**(3), 405-427.

Li, R., Ge, H. and Maruyama, R. (2017), "Assessment of post-earthquake serviceability for steel arch bridges with seismic dampers considering mainshock-aftershock sequences", *Earthq. Struct.*, **13**(2), 137-150.

Li, Y., Song, R. and Lindt, J.W.V.D. (2014), "Collapse fragility of steel structures subjected to earthquake mainshock-aftershock sequences", *J. Struct. Eng.*, **140**(12), 04014095.

Liu, Y., Paolacci, F. and Lu, D.G. (2017), "Seismic fragility of a typical bridge using extrapolated experimental damage limit states", *Earthq. Struct.*, **13**(6), 599-611.

Luco, N., Bazzurro, P. and Cornell, C.A. (2004), "Dynamic versus static computation of the residual capacity of a mainshock-damaged building to withstand an aftershock", *13th World Conference on Earthquake Engineering*.

Mazzoni, S., Mckenna, F., Scott, M.H. and Fenves, G.L. (2006), *Opensees Command Language Manual*, Pacific Earthquake Engineering Research (PEER) Center.

Nazari, N., Van De Lindt, J. and Li, Y. (2013), "Effect of mainshock-aftershock sequences on woodframe building damage fragilities", *J. Perform. Constr. Facil.*, **29**(1), 04014036.

Papaloizou, L., Polycarpou, P., Komodromos, P., Hatzigeorgiou, G.D. and Beskos, D.E. (2016), "Two-dimensional numerical investigation of the effects of multiple sequential earthquake excitations on ancient multi-drum columns", *Earthq. Struct.*, **10**(3), 495-521.

Polese, M., Di Ludovico, M., Prota, A. and Manfredi, G. (2013), "Damage-dependent vulnerability curves for existing buildings", *Earthq. Eng. Struct. Dyn.*, **42**(6), 853-870.

Raghunandan, M., Liel, A.B. and Luco, N. (2015), "Aftershock collapse vulnerability assessment of reinforced concrete frame structures", *Earthq. Eng. Struct. Dyn.*, **44**(3), 419-439.

Ruiz-García, J. and Aguilar, J.D. (2017), "Influence of modeling assumptions and aftershock hazard level in the seismic response of post-mainshock steel framed buildings", *Eng. Struct.*, **140**(437-446).

Ryu, H., Luco, N., Uma, S. and Liel, A. (2011), "Developing fragilities for mainshock-damaged structures through incremental dynamic analysis", *Ninth Pacific Conference on Earthquake Engineering*, Auckland, New Zealand.

Tang, Z., Xie, X. and Wang, T. (2016), "Residual seismic performance of steel bridges under earthquake sequence", *Earthq. Struct.*, **11**(4), 649-664.

Tesfamariam, S., Goda, K. and Mondal, G. (2015), "Seismic vulnerability of reinforced concrete frame with unreinforced masonry infill due to main shock–aftershock earthquake sequences", *Earthq. Spectra*, **31**(3), 1427-1449.

Uma, S., Ryu, H., Luco, N., Liel, A. and Raghunandan, M. (2011), "Comparison of main-shock and aftershock fragility curves developed for new zealand and us buildings", *Proceedings of the 9th Pacific Conference on Earthquake Engineering Structure Building and Earthquake-Resilient Society*, Auckland, New Zealand.

Vamvatsikos, D. and Allin Cornell, C. (2006), "Direct estimation of the seismic demand and capacity of oscillators with multi-linear static pushovers through ida", *Earthq. Eng. Struct. Dyn.*, **35**(9), 1097-1117.

Yu, X.H., Li, S., Lu, D.G. and Tao, J (2018), "Collapse capacity of inelastic single-degreeof-freedom systems subjected to mainshockaftershock earthquake sequences", *J. Earthq. Eng.*, 1-24.

Zhai, C.H., Wen, W.P., Li, S., Chen, Z., Chang, Z. and Xie, L.L. (2014), "The damage investigation of inelastic sdof structure under the mainshock-aftershock sequence-type ground motions", *Soil Dyn. Earthq. Eng.*, **59**(30-41).

Zhu, R.G., Lu, D.G., Yu, X.H. and Wang, G.Y. (2017), "Conditional mean spectrum of aftershocks", *Bull. Seismol. Soc. Am.*, **107**(4), 1940-1953.

AT